

DETECTION OF HCO⁺ EMISSION TOWARD THE PLANETARY NEBULA K3-35

D. TAFOYA,^{1,2} Y. GÓMEZ,¹ G. ANGLADA,³ L. LOINARD,¹ J. M. TORRELLES,⁴ L. F. MIRANDA,³ M. OSORIO,³
R. FRANCO-HERNÁNDEZ,^{1,2} L.-Å. NYMAN,⁵ J. NAKASHIMA,⁶ AND S. DEGUCHI⁷

Received 2006 July 31; accepted 2006 September 27

ABSTRACT

We report the detection, for the first time, of HCO⁺($J = 1 \rightarrow 0$) emission, as well as marginal CO($J = 1 \rightarrow 0$) emission, toward the planetary nebula (PN) K3-35 as a result of a molecular survey carried out toward this source. We also report new observations of the previously detected CO($J = 2 \rightarrow 1$) and water maser emission, as well as upper limits for the emission of the SiO, H¹³CO⁺, HNC, HCN, HC₃OH, HC₃N, CS, HC₃N, ¹³CO, CN, and NH₃ molecules. From the ratio of CO($J = 2 \rightarrow 1$) to CO($J = 1 \rightarrow 0$) emission we have estimated the kinetic temperature of the molecular gas, obtaining a value of $\simeq 20$ K. Using this result we have estimated a molecular mass for the envelope of $\simeq 0.017 M_{\odot}$ and an HCO⁺ abundance relative to H₂ of 6×10^{-7} , similar to the abundances found in other PNe. K3-35 is remarkable because it is one of the two PNe reported to exhibit water maser emission, which is present in the central region, as well as at a distance of $\simeq 5000$ AU from the center. The presence of molecular emission provides some clues that could help in understanding the persistence of water molecules in the envelope of K3-35. The HCO⁺ emission could be arising in dense molecular clumps, which may provide the shielding mechanism that protects water molecules in this source.

Key words: circumstellar matter — ISM: molecules — planetary nebulae: general — radio lines: ISM — stars: individual (K3-35)

1. INTRODUCTION

The chemical composition of the molecular envelope that surrounds a young planetary nebula (PN) can reflect the recent history of the transition from the asymptotic giant branch (AGB) to the PN phase. When envelopes of AGB stars are oxygen-rich, they may produce strong maser emission of one or more molecules, such as OH, H₂O, or SiO, which commonly appears stratified, with the SiO masers located close to the stellar surface, water masers in the range of about 10–100 AU, and OH masers farther away, up to 10⁴ AU from the central star (Reid & Moran 1981; Chapman & Cohen 1986).

Molecules that were present in the red giant envelope are destroyed by the radiation of the core as the star evolves to the PN phase, while other molecular species could develop in these peculiar physical conditions. In particular, water vapor masers that are detected in the giant envelopes (Reid & Moran 1981; Elitzur 1992; Habing 1996) and in some proto-PNe (Likkel & Morris 1988; Marvel & Boboltz 1999; Gómez & Rodríguez 2001; Imai et al. 2002) are not expected to persist in the PN phase, in which the envelope not only begins to be ionized but also becomes rare-

fied (Lewis 1989; Gómez et al. 1990). As the slow and massive mass loss of the late AGB phase stops and the star enters its PN phase, the water molecules are expected to disappear in a time-scale of decades (Gómez et al. 1990), and only OH masers seem to persist for a considerable time ($\simeq 1000$ yr; Kwok 1993). However, two PNe (K3-35 and IRAS 17347–3139; Miranda et al. 2001; de Gregorio-Monsalvo et al. 2004) have recently been found to harbor water maser emission, suggesting that these objects are in an early stage of their evolution as PNe, in which the physical and chemical conditions could still permit the existence of water molecules.

K3-35 is a very young PN (which evolved from an oxygen-rich AGB star) characterized by an S-shaped radio continuum emission morphology with a well-defined point-symmetric structure (Aaquist & Kwok 1989; Aaquist 1993; Miranda et al. 2000, 2001). The detected water vapor masers are located at the center of the nebula, apparently tracing a torus-like structure with a radius of $\simeq 85$ AU (adopting a distance of $\simeq 5$ kpc; Zhang 1995), and, in addition, they are also found at the surprisingly large distance of 5000 AU from the star, in the tips of the bipolar lobes (Miranda et al. 2001; Gómez et al. 2003). Water masers were not expected to be found at such an enormous distance in an evolved star, since the physical conditions required to pump the maser emission ($n_{\text{H}_2} \simeq 10^8 \text{ cm}^{-3}$, $T_k \simeq 500$ K) are difficult to explain, given our current understanding of these objects. Miranda et al. (2001) proposed that shocks driven by the bipolar jet could create the physical conditions necessary to pump the distant water vapor masers. However, the presence and persistence of water molecules in these PNe are still puzzling, probably being related to some shielding mechanism due to the presence of high-density molecular gas that protects water molecules against the ionizing radiation of the central star.

To investigate the possible existence of such a shielding mechanism, one must characterize the physical conditions of the molecular gas in the envelope surrounding K3-35. Interestingly, weak, broad CO($J = 2 \rightarrow 1$) emission has been detected toward K3-35 by Dayal & Bieging (1996) and, more recently, by Huggins

¹ Centro de Radioastronomía y Astrofísica, UNAM, Morelia, Michoacán, Mexico; d.tafoya@astrosmo.unam.mx, y.gomez@astrosmo.unam.mx, l.loinard@astrosmo.unam.mx, r.franco@astrosmo.unam.mx.

² Harvard-Smithsonian Center for Astrophysics, Cambridge, MA, USA; dtafoya@cfa.harvard.edu, rfranco@cfa.harvard.edu.

³ Instituto de Astrofísica de Andalucía, CSIC, Granada, Spain; guillem@iaa.es, lfm@iaa.es, osorio@iaa.es.

⁴ Facultat de Física, Institut de Ciències del Espai and Institut d'Estudis Espacials de Catalunya, Universitat de Barcelona, Barcelona, Spain; torrelles@ieec.fcr.es.

⁵ Swedish-ESO Submillimetre Telescope, European Southern Observatory, Santiago, Chile; and Onsala Space Observatory, Onsala, Sweden; lnyman@eso.org.

⁶ Institute of Astronomy and Astrophysics, Academia Sinica, Taipei, Taiwan; junichi@asiaa.sinica.edu.tw.

⁷ Department of Astronomical Science, Graduate University for Advanced Studies, Nobeyama Observatory, Minamimaki, Minamisaku, Nagano, Japan; deguchi@nro.nao.ac.jp.

TABLE 1
 SINGLE-DISH OBSERVATIONS TOWARD K3-35

Molecule	Transition	Frequency (GHz)	$\eta_{\text{MB}}^{\text{a}}$	Γ^{b} (K Jy ⁻¹)	$\Delta\text{ch}^{\text{c}}$ (km s ⁻¹)	rms (T_{MB}^{d}) (K)	$\int T_{\text{MB}} dv^{\text{e}}$ (K km s ⁻¹)	$v_{\text{LSR}}^{\text{f}}$ (km s ⁻¹)	Δv^{g} (km s ⁻¹)
20 m OSO, 2003 February–March									
SiO	$v = 1, J = 2 \rightarrow 1$	86.2434420	0.65	0.045	0.174	0.024
H ¹³ CO ⁺	$J = 1 \rightarrow 0$	86.7542940	0.64	0.045	0.173	0.024
HCN	$J = 1 \rightarrow 0, F = 2 \rightarrow 1$	88.6318473	0.63	0.043	0.169	0.017
HCO ⁺	$J = 1 \rightarrow 0$	89.1885180	0.63	0.043	0.168	0.012	0.33 ± 0.03	28	20
HNC	$J = 1 \rightarrow 0, F = 2 \rightarrow 1$	90.6635430	0.61	0.043	0.165	0.024
CH ₃ OH	$J = 8_0 \rightarrow 7_1 A^+$	95.1694400	0.58	0.040	0.158	0.028
HC ₅ N	$J = 36 \rightarrow 35$	95.8503370	0.58	0.040	0.156	0.030
CS	$J = 2 \rightarrow 1$	97.9809680	0.56	0.038	0.153	0.027
HC ₃ N	$J = 12 \rightarrow 11$	109.173634	0.47	0.034	0.137	0.039
¹³ CO	$J = 1 \rightarrow 0$	110.201353	0.47	0.033	0.068	0.045
CN	$J = 1 \rightarrow 0$	113.490982	0.44	0.032	0.132	0.044
45 m Nobeyama, 2003 March 9									
H ₂ O	$J = 6_{16} \rightarrow 5_{23}$	22.235080	0.81	0.357	0.250	0.010	1.5 ± 0.1	21.4	0.72
	0.250	0.010	1.6 ± 0.1	22.5	0.88
NH ₃	$(J, K) = (1, 1)$	23.695110	0.81	0.357	0.250	0.010
CO	$J = 1 \rightarrow 0$	115.271204	0.46	0.196	0.083	0.200	2.7 ± 0.4	27	10
30 m IRAM, 2003 April 1									
CO	$J = 2 \rightarrow 1$	230.537990	0.58	0.105	0.406	0.088	10.2 ± 0.4	23	20

^a Main-beam efficiency. The main-beam brightness temperature is obtained as $T_{\text{MB}} = T'_A/\eta_{\text{MB}}$, where T'_A is the antenna temperature corrected for the atmospheric attenuation.

^b Sensitivity of the telescope. The flux density can be obtained as $S_\nu = \eta_{\text{MB}} T_{\text{MB}}/\Gamma$.

^c Channel width.

^d The 1 σ rms noise per channel (in T_{MB} scale).

^e Zero-order moment (velocity-integrated intensity) of the line emission.

^f First-order moment (intensity-weighted mean v_{LSR}) of the line emission.

^g Equivalent line width, obtained from the second-order moment. For a Gaussian line profile, this value corresponds to the FWHM.

et al. (2005), indicating the presence of a neutral molecular envelope and suggesting the possible presence of dense molecular clumps. In this paper we present a search for additional molecular emission toward K3-35, reporting the first detection of HCO⁺ in this PN, confirmation of CO($J = 2 \rightarrow 1$) and water maser emission, and a tentative detection of CO($J = 1 \rightarrow 0$).

2. OBSERVATIONS

The survey for molecular lines toward the young PN K3-35 was carried out using the Onsala 20 m telescope in Sweden, the 45 m Nobeyama telescope in Japan, and the IRAM 30 m telescope in Spain (see Table 1). The coordinates R.A. (J2000.0) = 19^h27^m44^s, decl. (J2000.0) = 21°30′03″ were adopted for the position of K3-35 (Miranda et al. 2001). In the following subsections we describe each of these observations.

2.1. 20 m Onsala

Observations of several molecular transitions from 86 to 113 GHz were carried out using the 20 m telescope of the Onsala Space Observatory (OSO)⁸ in the dual beam-switching mode. We used a 100 GHz receiver, which includes a cryogenically cooled SIS mixer covering the frequency range from 84 to 116 GHz. The back end used was the LCOR autocorrelator, which, for all molecular transitions except for ¹³CO, had a bandwidth of 80 MHz, providing a resolution of 50 kHz. This corresponds to a velocity resolution of $\simeq 0.17$ km s⁻¹ at 86 GHz and $\simeq 0.13$ km s⁻¹ at

115 GHz. The ¹³CO observations were carried out with a bandwidth of 40 MHz, providing a spectral resolution of 25 kHz, which corresponds to a velocity resolution of $\simeq 0.068$ km s⁻¹. In all cases the bandwidth was centered at $v_{\text{LSR}} = 20$ km s⁻¹. The half-power beam width (HPBW) of the telescope ranges from $\simeq 44''$ at 86 GHz to $33''$ at 115 GHz. System temperatures were typically in the range from 300 to 500 K. The parameters of the molecular transitions observed, as well as additional telescope parameters, are given in Table 1.

2.2. 45 m Nobeyama

Observations with the 45 m radio telescope at Nobeyama⁹ were carried out using the position-switching mode. The Beam Array Receiver System, consisting of a grid of 5 × 5 beams separated by $\sim 41''$, was used for the observations of the CO($J = 1 \rightarrow 0$) transition at 115 GHz. The back-end bandwidth was 32 MHz and was centered at $v_{\text{LSR}} = 20$ km s⁻¹, providing a spectral resolution of 30 kHz ($\simeq 0.08$ km s⁻¹). The HPBW of the telescope at this frequency is $\simeq 16''$. Typical system temperatures for the 115 GHz observations were in the 420–450 K range.

Observations of the H₂O maser and NH₃(1,1) lines at $\nu \simeq 22$ –24 GHz were carried out using the H22 receiver. We used a bandwidth of 40 MHz centered at $v_{\text{LSR}} = 20$ km s⁻¹ with a frequency resolution of 20 kHz ($\simeq 0.25$ km s⁻¹). The HPBW of the telescope at these frequencies is $\sim 70''$. Typical system temperatures

⁸ Onsala Space Observatory at Chalmers University of Technology is the Swedish National Facility for Radio Astronomy.

⁹ The Nobeyama Radio Observatory is a branch of the National Astronomical Observatory, an interuniversity research institute, operated by the Ministry of Education, Science, and Culture, Japan.

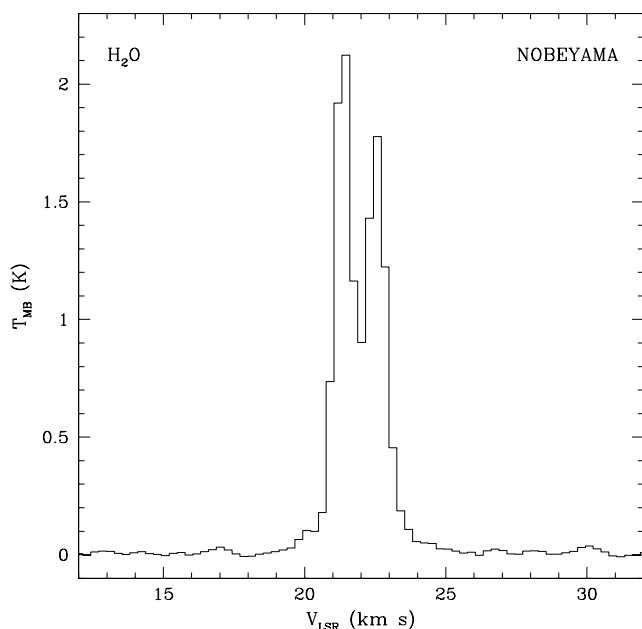


FIG. 1.—Water maser spectrum toward K3-35 observed on 2003 March 9 with the Nobeyama 45 m telescope. The spectrum has been smoothed to a resolution of 0.25 km s^{-1} , and a first-order polynomial baseline has been subtracted. The rms noise in the offline channels is 0.01 K . Two components at LSR velocities of 21.4 and 22.5 km s^{-1} can be identified.

for these observations were $200\text{--}300 \text{ K}$. The parameters of the molecular transitions observed, as well as additional telescope parameters, are given in Table 1.

2.3. 30 m IRAM

Observations of the $\text{CO}(J = 2 \rightarrow 1)$ line at 230 GHz were carried out with the IRAM 30 m telescope at Pico Veleta using the position-switching mode. We used the multibeam Heterodyne Receiver Array (HERA), which consists of nine receivers arranged in a regular 3×3 grid with spacing on the sky of $24''$, and a beam size of $\sim 12''$. The back end used was the Versatile Spectral and Polarimetric Array autocorrelator split into two parts, providing 438 channels of 0.41 km s^{-1} width and 224 channels of 1.63 km s^{-1} width for each of the nine receivers. The system temperature was $\sim 300 \text{ K}$, and the pointing uncertainty was $\sim 2''$. The parameters of the molecular transition observed, as well as additional telescope parameters, are given in Table 1.

3. RESULTS

In Table 1 we summarize the results of our molecular survey toward K3-35. We succeeded in detecting weak emission of $\text{HCO}^+(J = 1 \rightarrow 1)$ and $\text{CO}(J = 1 \rightarrow 0)$, both reported for the first time in this work. We also detected $\text{CO}(J = 2 \rightarrow 1)$ emission, which was reported previously by Dayal & Bieging (1996) and Huggins et al. (2005), and water maser emission, reported previously by Engels et al. (1985), Miranda et al. (2001), and de Gregorio-Monsalvo et al. (2004). The remaining molecular transitions listed in Table 1 have not been detected. The integrated intensity, central velocity, and line width of the detected lines are presented in Table 1, where we also give the rms achieved in all the transitions observed in our survey.

3.1. H_2O

Using the 45 m Nobeyama telescope we detected the $\text{H}_2\text{O}(J = 6_{16} \rightarrow 5_{23})$ maser line toward K3-35 (see Fig. 1 and Table 1). The maser emission appears in the velocity range from 20 to

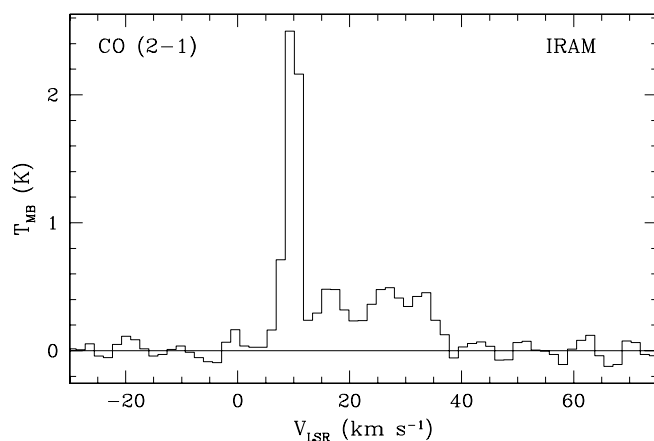


FIG. 2.— $\text{CO}(J = 2 \rightarrow 1)$ spectrum toward K3-35 observed with the IRAM 30 m telescope. The spectrum has been smoothed to a resolution of 1.6 km s^{-1} , and a second-order polynomial baseline has been subtracted. The emission has two velocity components, a narrow component ($\Delta v \simeq 5 \text{ km s}^{-1}$) centered at $v_{\text{LSR}} \simeq 10 \text{ km s}^{-1}$ and a broad component ($\Delta v \simeq 20 \text{ km s}^{-1}$) centered at $v_{\text{LSR}} \simeq 23 \text{ km s}^{-1}$.

24 km s^{-1} , with two clear components centered at $v_{\text{LSR}} = 21.4$ and 22.5 km s^{-1} , similar to the velocities of the strongest peaks observed by Engels et al. (1985) and Miranda et al. (2001). The Very Large Array observations of Miranda et al. (2001) reveal that this velocity range corresponds essentially to the features observed toward the center of K3-35 and the tip of its northern lobe.

3.2. CO

Using the IRAM 30 m telescope we have detected $\text{CO}(J = 2 \rightarrow 1)$ emission toward K3-35. The observed emission has two velocity components, a narrow component ($\Delta v \simeq 5 \text{ km s}^{-1}$) centered at $v_{\text{LSR}} \simeq 10 \text{ km s}^{-1}$ and a broad component ($\Delta v \simeq 20 \text{ km s}^{-1}$) centered at $v_{\text{LSR}} \simeq 23 \text{ km s}^{-1}$ (see Fig. 2). Our observations with the multibeam HERA array reveal that, while the emission of the narrow component is present over a large region ($\gg 1'$), the broad component is only detected toward the position of K3-35. Given its line width and angular extension, we conclude that the narrow component is probably of interstellar origin, while the broad component is most likely associated with the PN K3-35. In order to better isolate the CO emission associated with K3-35, a Gaussian fit to the narrow component was subtracted from the overall spectrum.

In Figure 3 we show the resulting $\text{CO}(J = 2 \rightarrow 1)$ spectrum toward K3-35, after subtraction of the narrow component. In Table 1 we give the line parameters of the broad component associated with K3-35. The values of the central velocity and line width are similar to those reported previously by Dayal & Bieging (1996) using the Kitt Peak 12 m telescope and, more recently, by Huggins et al. (2005) using the Pico Veleta 30 m telescope. Our line intensity is higher than the value reported by Huggins et al. (2005), and this can be due to slight differences in the pointing, given the small size of the 30 m beam at 1.3 mm . Figure 4 shows a $\text{CO}(J = 2 \rightarrow 1)$ spectra mosaic (after subtraction of the narrow component at 10 km s^{-1}) of a region of $1' \times 1'$, centered on K3-35. This mosaic shows that broad emission is coming from within a region smaller than $\sim 20''$, providing a constraint on the angular size of the K3-35 molecular envelope.

We also have detected weak, broad $\text{CO}(J = 1 \rightarrow 0)$ emission toward K3-35 using the Nobeyama 45 m telescope (see Fig. 3 [bottom] and Table 1). An interstellar narrow $\text{CO}(J = 1 \rightarrow 0)$ component was also present and subtracted as in the

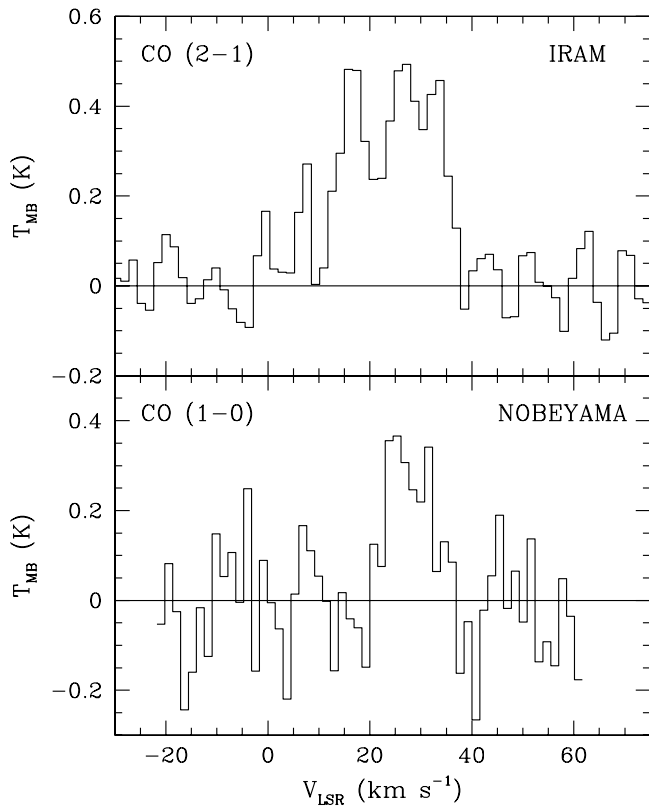


FIG. 3.—*Top*: CO($J = 2 \rightarrow 1$) spectrum toward K3-35 observed with the IRAM 30 m telescope. The spectrum has been smoothed to a resolution of 1.6 km s^{-1} , and a second-order polynomial baseline has been subtracted. The narrow interstellar component at $v_{\text{LSR}} \simeq 10 \text{ km s}^{-1}$ (Fig. 2) has also been subtracted (see § 3.2). The rms noise in the offline channels is $\sim 0.063 \text{ K}$. The line emission is centered at $v_{\text{LSR}} \simeq 23 \text{ km s}^{-1}$, with a line width of $\Delta v \simeq 20 \text{ km s}^{-1}$. *Bottom*: CO($J = 1 \rightarrow 0$) spectrum toward K3-35 observed with the Nobeyama 45 m telescope. The spectrum has been smoothed to a resolution of 1.5 km s^{-1} , and a third-order polynomial baseline has been subtracted. The narrow interstellar component at $v_{\text{LSR}} \simeq 10 \text{ km s}^{-1}$ has also been subtracted. The rms noise in the offline channels is $\sim 0.1 \text{ K}$. The line emission is centered at $v_{\text{LSR}} \simeq 27 \text{ km s}^{-1}$, with a line width of $\Delta v \simeq 10 \text{ km s}^{-1}$.

CO($J = 2 \rightarrow 1$) data. The central velocity of the broad emission is $v_{\text{LSR}} \simeq 27 \text{ km s}^{-1}$, and the line width is $\Delta v \simeq 10 \text{ km s}^{-1}$. This is the first time that the CO($J = 1 \rightarrow 0$) transition has been reported in association with this PN. Although the line is only marginally detected (3σ) and more sensitive observations are necessary to confirm the detection, it is located at the right velocity, suggesting a true association with K3-35. We attribute the apparent difference in line widths between the CO($J = 2 \rightarrow 1$) and CO($J = 1 \rightarrow 0$) lines to the modest signal-to-noise ratio of the CO($J = 1 \rightarrow 0$) detection.

The CO emission is very useful for investigating the physical parameters of the molecular gas associated with the PN K3-35. An estimate of the kinetic temperature of the gas can be obtained from the ratio of the CO($J = 2 \rightarrow 1$) to CO($J = 1 \rightarrow 0$) transitions. Assuming that the level populations are well thermalized and that the emission is optically thin, and neglecting the correction for departures from the Rayleigh-Jeans regime, the kinetic temperature can be approximated by the following equation:

$$T_k = -\frac{11.06}{\ln(R/4)}, \quad (1)$$

where R is the ratio of the CO($J = 2 \rightarrow 1$) to CO($J = 1 \rightarrow 0$) velocity integrated line intensities corrected by the difference in

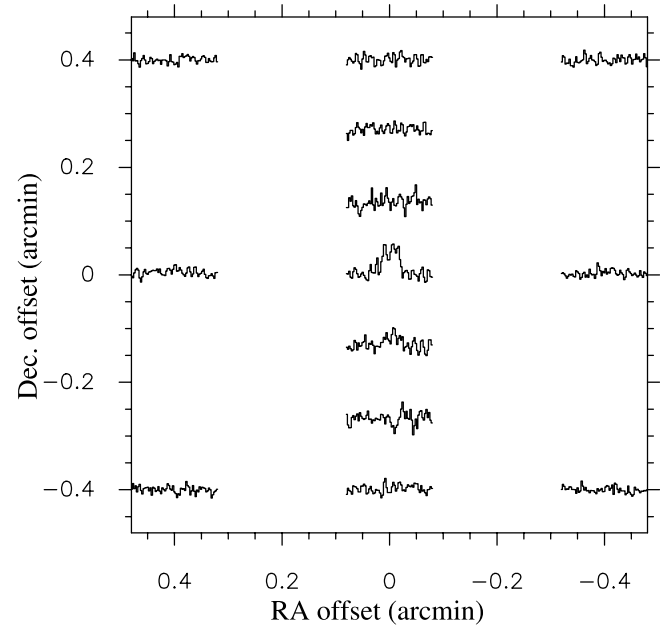


FIG. 4.—Mosaic of CO($J = 2 \rightarrow 1$) spectra in the region around K3-35 obtained with the IRAM 30 m telescope. A narrow interstellar component at $v_{\text{LSR}} \simeq 10 \text{ km s}^{-1}$, present in all the positions, has been subtracted from the spectra. The (0, 0) offset position corresponds to the position of K3-35, R.A. (J2000.0) = $19^{\text{h}}27^{\text{m}}44^{\text{s}}$, decl. (J2000.0) = $21^{\circ}30'03''$. Note that the emission arises from a compact region toward K3-35.

beam sizes. If the emission is unresolved in both transitions, $R = (\theta_{2 \rightarrow 1} / \theta_{1 \rightarrow 0})^2 \int T_{\text{MB}}(\text{CO}; 2 \rightarrow 1) dv / \int T_{\text{MB}}(\text{CO}; 1 \rightarrow 0) dv$, where θ is the FWHM of the telescope main beam. Using the integrated intensities of our 30 and 45 m CO observations, we derived a value of $20 \pm 6 \text{ K}$ for the kinetic temperature of the molecular gas in K3-35. Analysis of previous observations led to a higher kinetic temperature estimate ($T_k \geq 120 \text{ K}$; Dayal & Bieging 1996). However, from our observations, and taking properly into account the difference in the telescope beam sizes, for K3-35 we derive a lower value for the kinetic temperature that is more similar to other kinetic temperature determinations in young PNe, typically ranging from 25 to 60 K (Bachiller et al. 1997).

The CO column density and molecular mass can also be derived from the CO observations, assuming LTE conditions and that the emission is optically thin. For this we use the CO($J = 2 \rightarrow 1$) line, since its spectrum is of better quality (see Fig. 3). The beam-averaged CO column density can be obtained using the following relation:

$$\left[\frac{N(\text{CO})}{\text{cm}^{-2}} \right] = \frac{1.1 \times 10^{13} T_k}{(e^{-5.54 \text{ K}/T_k} - e^{-16.60 \text{ K}/T_k}) \left[(e^{11.06 \text{ K}/T_k} - 1)^{-1} - 0.02 \right]} \times \left[\frac{\int T_{\text{MB}}(\text{CO}; 2 \rightarrow 1) dv}{\text{K km s}^{-1}} \right]. \quad (2)$$

For a kinetic temperature $T_k = 20 \text{ K}$, we obtain a beam-averaged CO column density $N(\text{CO}) = 5.1 \times 10^{15} \text{ cm}^{-2}$ for the K3-35 envelope. The result is weakly dependent on the precise value of T_k adopted [for $T_k \simeq 100 \text{ K}$, $N(\text{CO})$ would be only a factor of 2.6 higher].

The molecular mass of the envelope can be estimated using the following expression:

$$\left(\frac{M_m}{M_{\odot}} \right) = 2.9 \times 10^{-25} \left(\frac{\theta}{\text{arcsec}} \right)^2 \left(\frac{D}{\text{kpc}} \right)^2 \left[\frac{N(\text{CO})}{\text{cm}^{-2}} \right] X_{\text{CO}}^{-1}, \quad (3)$$

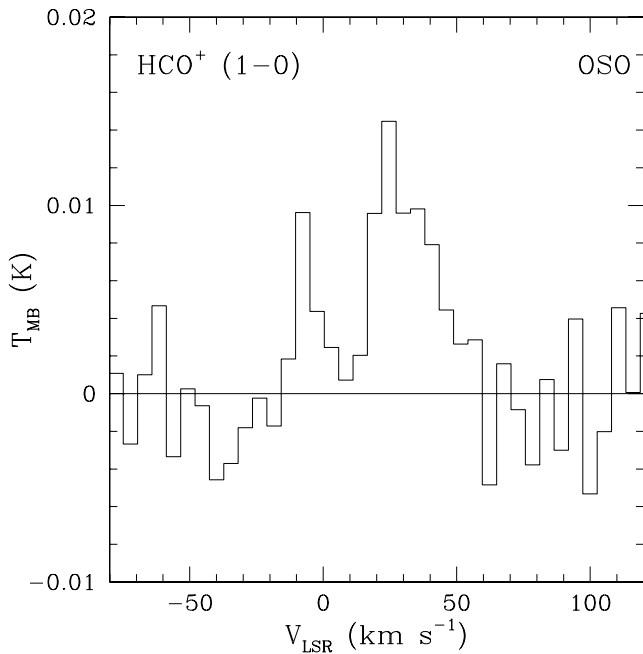


FIG. 5.— $\text{HCO}^+(J = 1 \rightarrow 0)$ spectrum toward K3-35 observed with the Onsala 20 m telescope. The spectrum has been smoothed to a resolution of 5.4 km s^{-1} , and a second-order polynomial baseline has been subtracted. The rms noise in the offline channels is $\sim 0.003 \text{ K}$. The line emission is centered at $v_{\text{LSR}} \simeq 28 \text{ km s}^{-1}$, with a line width of $\Delta v \simeq 20 \text{ km s}^{-1}$.

where θ is the FWHM of the telescope beam, D is the distance to the source, and X_{CO} is the abundance of CO relative to H_2 . Using a representative value for PNe, $X_{\text{CO}} \simeq 3 \times 10^{-4}$ (Huggins et al. 1996), and adopting a distance of $D = 5 \text{ kpc}$ to K3-35, we estimate a molecular mass for the envelope of $M_m \simeq 0.017 M_{\odot}$. This result can be easily scaled for different values of T_k , D , and X_{CO} using the expressions given above.

3.3. HCO^+

$\text{HCO}^+(J = 1 \rightarrow 0)$ emission was detected toward K3-35 with the 20 m Onsala telescope. This is the first time that HCO^+ emission has been reported in association with this PN. The observed spectrum is shown in Figure 5, and the line parameters are given in Table 1. The mean velocity of the HCO^+ emission is $v_{\text{LSR}} \simeq 28 \text{ km s}^{-1}$, and the line width is $\Delta v \simeq 20 \text{ km s}^{-1}$. These values are similar to those obtained from the $\text{CO}(J = 2 \rightarrow 1)$ observations reported by Dayal & Bieging (1996), Huggins et al. (2005), and in the present work, supporting the idea that the detected HCO^+ emission is associated with the PN K3-35.

Assuming LTE conditions and that the emission is optically thin, we can estimate the beam-averaged HCO^+ column density from our observations using the following equation:

$$\left[\frac{N(\text{HCO}^+)}{\text{cm}^{-2}} \right] = \frac{7.9 \times 10^{10} T_k}{(1 - e^{-4.29 \text{ K}/T_k}) \left[(e^{4.29 \text{ K}/T_k} - 1)^{-1} - 0.26 \right]} \times \left[\frac{\int T_{\text{MB}}(\text{HCO}^+; 1 \rightarrow 0) dv}{\text{K km s}^{-1}} \right]. \quad (4)$$

For a kinetic temperature $T_k = 20 \text{ K}$, the resulting beam-averaged HCO^+ column density is $N(\text{HCO}^+) \simeq 6.9 \times 10^{11} \text{ cm}^{-2}$. For K3-35 this value implies an HCO^+ abundance relative to CO, $[\text{HCO}^+/\text{CO}] = 1.9 \times 10^{-3}$, where we have corrected for the difference in the beam sizes, and an HCO^+ abundance relative to H_2 , $X_{\text{HCO}^+} = 5.7 \times 10^{-7}$, assuming that $X_{\text{CO}} = 3 \times 10^{-4}$.

4. DISCUSSION

The presence of water maser emission led to the suggestion that K3-35 is an extremely young PN (Miranda et al. 2001), given that water molecules are expected to survive for only a short time ($\lesssim 100 \text{ yr}$) during the PN phase. However, the existence of these molecules in the envelope may not be an unambiguous indicator of youth, since dense molecular clumps could be protecting the water molecules from photodissociation and letting them survive for a longer time. An alternative way to probe the evolutionary status of PNe is to analyze their molecular content. It is known that the molecular abundances in protoplanetary nebula (PPN) envelopes change as the core begins to produce UV radiation and the star enters the PN phase. In particular, it has been observed that the HCO^+ abundance increases rapidly when the star goes from the PPN to PN phase (Bachiller et al. 1997; Josselin & Bachiller 2003), providing some indications of the evolutionary state. Furthermore, Huggins et al. (1996) found that the ratio of molecular to ionized mass, M_m/M_i , is inversely correlated with the radius of the nebula; therefore, it can be taken as an indicator of the evolutionary stage of the PN, almost independent of the distance.

In order to probe the evolutionary status of K3-35 and compare it with other objects, we estimated the ratio M_m/M_i for K3-35. The molecular mass for K3-35 was obtained from our results in § 3.2. To estimate the mass of ionized gas in K3-35, we have followed the formulation of Mezger & Henderson (1967) and used the 3.6 cm radio continuum data of Miranda et al. (2001). The value for the ionized mass is $M_i \simeq 9 \times 10^{-3} M_{\odot}$, resulting in a ratio of molecular to ionized mass $M_m/M_i \simeq 1.9$ for K3-35. This value for the ratio of molecular to ionized mass in K3-35 is comparable to the values found for other young PNe (e.g., IC 5117) with kinematical ages of a few hundred years (Miranda et al. 1995). In order to further test the evolutionary status of K3-35, we plot in Figure 6 the HCO^+ abundance as a function of the ratio

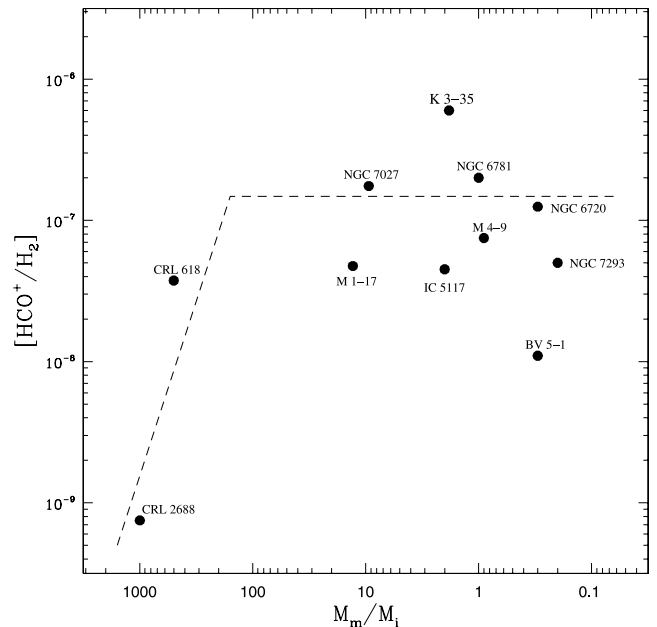


FIG. 6.— HCO^+ abundance as a function of the ratio between molecular and ionized mass for several PPNs and PNe. The M_m/M_i ratio has been found to decrease with the age of the PN (Huggins et al. 1996). Therefore, the plot illustrates the time evolution of the HCO^+ abundance. The dashed line represents the average HCO^+ abundance for PPNs and PNe. Note the significant increase in the HCO^+ abundance from the PPN to the PN phase. Data points are taken from Bachiller et al. (1997) and Josselin & Bachiller (2003), except for K3-35 (this work).

of molecular to ionized mass for K3-35, as well as for a sample of PNe and PNe taken from Bachiller et al. (1997) and Josselin & Bachiller (2003). Figure 6 shows that the HCO⁺ abundance in K3-35 is ~ 500 times higher than the abundance in the PPN CRL 2688, and that it has reached a value comparable to (in fact, somewhat higher than) those found in more evolved PNe.

The HCO⁺ traces molecular gas with densities of order of $\sim 10^5$ cm⁻³, such as that forming dense molecular clumps embedded in the ionized material (Huggins et al. 1992). It is feasible that these clumps could be protecting other molecules, such as H₂O, from the ionizing radiation. Therefore, the detection of HCO⁺ in K3-35 suggests that dense molecular clumps could be responsible for the shielding of the water molecules present in this nebula. Higher angular resolution observations at millimeter and submillimeter wavelengths would be very valuable to confirm the clumpiness in K3-35.

In summary, our study of K3-35 indicates that the molecular data on this PN are consistent with this source being a relatively young (a few hundred years) PN, in which the survival of water molecules may be favored by the presence of dense molecular clumps that could be protecting the water molecules from photodissociation.

5. CONCLUSIONS

We have carried out a survey for molecular emission toward the young planetary nebula (PN) K3-35. As a result of this survey, we detected for the first time HCO⁺($J = 1 \rightarrow 0$) and CO($J = 1 \rightarrow 0$) emission toward this PN. The emission appears in a velocity range that is in agreement with that of the broad CO($J = 2 \rightarrow 1$) emission reported in previous studies, as well as in the present work. We have also mapped the CO($J = 2 \rightarrow 1$) line, showing that the emission is compact and centered on K3-35, confirming the association with the PN, and setting an upper limit for the angular size of the molecular envelope around K3-35

of $\lesssim 20''$. We have used the ratio of the CO($J = 2 \rightarrow 1$) and CO($J = 1 \rightarrow 0$) lines to obtain a better-constrained estimate of the kinetic temperature in the K3-35 molecular envelope, which turns out to be $\sim 20 \pm 6$ K. From our observations we have found that the HCO⁺ abundance in K3-35 is $\sim 6 \times 10^{-7}$, which is similar to values found in other young PNe. This result, along with the value for the ratio of molecular to ionized mass, $M_m/M_i \simeq 1.9$, suggests that K3-35 might not be an extremely young (< 100 yr) PN but a somewhat more evolved one (a few hundred years) in which the presence of water maser emission could be favored by a shielding mechanism that prevents the water molecules from being dissociated. Since it is believed that the HCO⁺ emission could be arising in dense clumps of molecular material embedded in the ionized gas, its detection in K3-35, a source of water maser emission, provides an important clue to understanding the shielding mechanism that could be protecting the water molecules from the radiation of the central star. Interferometric molecular observations at millimeter and submillimeter wavelengths would be very valuable to determine the morphology of the molecular envelope and to investigate the clumpiness of the HCO⁺ emission in this remarkable young PN.

R. F.-H., Y. G., L. L., and D. T. acknowledge support from DGAPA, UNAM, and CONACYT, Mexico. G. A., M. O., and J. M. T. acknowledge partial financial support from grant AYA 2005-08523-C03 of the Spanish MEC (cofounded with FEDER funds). L. F. M. is supported partially by grant AYA 2005-01495 of the Spanish MEC (cofounded with FEDER funds). G. A., M. O., and L. F. M. acknowledge support from Junta de Andalucía. J. M. T. acknowledges the warm hospitality of the UK Astronomy Technology Centre, Royal Observatory Edinburgh, during his sabbatical stay.

REFERENCES

- Aaquist, O. B. 1993, *A&A*, 267, 260
 Aaquist, O. B., & Kwok, S. 1989, *A&A*, 222, 227
 Bachiller, R., Forveille, T., Huggins, P. J., & Cox, P. 1997, *A&A*, 324, 1123
 Chapman, J. M., & Cohen, R. J. 1986, *MNRAS*, 220, 513
 Dayal, A., & Bieging, J. H. 1996, *ApJ*, 472, 703
 de Gregorio-Monsalvo, I., Gómez, Y., Anglada, G., Cesaroni, R., Miranda, L. F., Gómez, J. F., & Torrelles, J. M. 2004, *ApJ*, 601, 921
 Elitzur, M. 1992, *ARA&A*, 30, 75
 Engels, D., Schmid-Burgk, J., Walmsley, C. M., & Winnberg, A. 1985, *A&A*, 148, 344
 Gómez, Y., Miranda, L. F., Anglada, G., & Torrelles, J. M. 2003, in *IAU Symp.* 209, *Planetary Nebulae: Their Evolution and Role in the Universe*, ed. S. Kwok, M. Dopita, & R. Sutherland (San Francisco: ASP), 263
 Gómez, Y., Moran, J. M., & Rodríguez, L. F. 1990, *Rev. Mex. AA*, 20, 55
 Gómez, Y., & Rodríguez, L. F. 2001, *ApJ*, 557, L109
 Habing, H. J. 1996, *A&A Rev.*, 7, 97
 Huggins, P. J., Bachiller, R., Cox, P., & Forveille, T. 1992, *ApJ*, 401, L43
 ———. 1996, *A&A*, 315, 284
 Huggins, P. J., Bachiller, R., Planesas, P., Forveille, T., & Cox, P. 2005, *ApJS*, 160, 272
 Imai, H., Obara, K., Diamond, P. J., Omodaka, T., & Sasao, T. 2002, *Nature*, 417, 829
 Josselin, E., & Bachiller, R. 2003, *A&A*, 397, 659
 Kwok, S. 1993, *ARA&A*, 31, 63
 Lewis, B. M. 1989, *ApJ*, 338, 234
 Likkell, L., & Morris, M. 1988, *ApJ*, 329, 914
 Marvel, K. B., & Boboltz, D. A. 1999, *AJ*, 118, 1791
 Mezger, P. G., & Henderson, A. P. 1967, *ApJ*, 147, 471
 Miranda, L. F., Fernández, M., Alcalá, J. M., Guerrero, M. A., Anglada, G., Gómez, Y., Torrelles, J. M., & Aaquist, O. B. 2000, *MNRAS*, 311, 748
 Miranda, L. F., Gómez, Y., Anglada, G., & Torrelles, J. M. 2001, *Nature*, 414, 284
 Miranda, L. F., Torrelles, J. M., & Eiroa, C. 1995, *ApJ*, 446, L39
 Reid, M. J., & Moran, J. M. 1981, *ARA&A*, 19, 231
 Zhang, C. Y. 1995, *ApJS*, 98, 659